



Available online at www.sciencedirect.com



C. R. Mécanique 332 (2004) 867–874



<http://france.elsevier.com/direct/CRAS2B/>

Computation of the mean velocity field above a stack plate in a thermoacoustic refrigerator

David Marx, Philippe Blanc-Benon

Centre acoustique, LMFA UMR 5509, École centrale de Lyon, 69134 Ecully cedex, France

Received 23 April 2004; accepted 6 July 2004

Available online 1 October 2004

Presented by Geneviève Comte-Bellot

Abstract

A numerical simulation of the unsteady flow above one stack plate in a thermoacoustic refrigerator was performed. The second order mean velocity field was computed. Two regions could be distinguished. In the first region, located at the plate extremities, the mean flow is essentially vortical and results from the resonator/plate transition. In the second region, located above the plate, the mean velocity field corresponds to a streaming flow which results from the interaction of the acoustic wave with the plate boundaries. The effects of stack plates spacing on the streaming flow pattern is studied. **To cite this article:** *D. Marx, Ph. Blanc-Benon, C. R. Mécanique 332 (2004).*

© 2004 Académie des sciences. Published by Elsevier SAS. All rights reserved.

Résumé

Simulation numérique de la vitesse moyenne près d'une plaque de l'empilement d'un réfrigérateur thermoacoustique. Le champ de vitesse moyen à proximité d'une plaque appartenant à l'empilement d'un réfrigérateur thermoacoustique a été calculé numériquement par une simulation directe des équations de Navier–Stokes. Deux zones ont pu être distinguées. Dans la première, située aux extrémités de la plaque, le champ de vitesse moyen est vortical et résulte de la transition plaque/résonateur. Dans la seconde, située au-dessus de la plaque, le mouvement moyen est de type « acoustic streaming » et résulte de l'interaction entre l'onde acoustique et la surface de la plaque. L'influence de la distance inter-plaques dans l'empilement sur la forme de ce mouvement est étudiée. **Pour citer cet article :** *D. Marx, Ph. Blanc-Benon, C. R. Mécanique 332 (2004).*

© 2004 Académie des sciences. Published by Elsevier SAS. All rights reserved.

Keywords: Computational fluid mechanics; Thermoacoustics; Streaming; Numerical simulation

Mots-clés : Mécanique des fluides numérique ; Thermoacoustique ; Streaming ; Simulation numérique

E-mail addresses: david.marx@ec-lyon.fr (D. Marx), philippe.blanc-benon@ec-lyon.fr (Ph. Blanc-Benon).

1631-0721/\$ – see front matter © 2004 Académie des sciences. Published by Elsevier SAS. All rights reserved.
doi:10.1016/j.crme.2004.07.010

Version française abrégée

Un réfrigérateur thermoacoustique [1] est représenté à la Fig. 1 : un empilement de plaques (ou « stack ») placé dans l'onde stationnaire d'un résonateur acoustique pompe de l'énergie de l'une de ses extrémités à l'autre. L'ajout d'échangeurs de chaleur de part et d'autre de l'empilement complète le dispositif, qui effectue un cycle de réfrigération sous l'influence de l'onde acoustique stationnaire. Des mouvements moyens du fluide sont susceptibles de venir modifier le comportement du réfrigérateur. Ces mouvements sont ici étudiés à proximité de l'empilement au moyen d'une simulation numérique.

La simulation est basée sur une résolution des équations de Navier–Stokes par utilisation d'un schéma de Runge–Kutta d'ordre quatre pour l'intégration temporelle, et de différences finies d'ordre quatre pour le calcul des dérivées spatiales [10]. Du fait de la périodicité de l'empilement dans la direction y , la simulation est faite sur un domaine de calcul CD restreint (Figs. 1 et 2) comprenant une seule plaque de l'empilement, cette plaque étant supposée d'épaisseur négligeable. La condition thermique à sa surface est isotherme ou adiabatique. La hauteur, y_0 , du domaine de calcul est égale à la moitié de la distance, $2y_0$, entre deux plaques dans l'empilement.

L'étude des mouvements moyens fait apparaître deux zones (Fig. 3). La première zone comprend le fluide situé à proximité des extrémités de la plaque. Dans cette zone les mouvements moyens sont des mouvements vorticaux dus au passage d'une condition de glissement à l'extérieur de la plaque à une condition d'adhérence sur la plaque. La deuxième zone est située au-dessus de la partie centrale de la plaque. Les mouvements moyens dans cette zone ont un module moins important que dans la première zone. Ils résultent de l'interaction de l'onde acoustique avec la surface de la plaque et sont connus sous le terme « acoustic streaming » en anglais, parfois traduit par « vent d'acoustique non-linéaire » en français. Le reste de l'étude leur est consacré.

L'étude de l'écoulement moyen entre deux parois sous l'influence d'une onde acoustique stationnaire remonte à Rayleigh [3], qui se base sur deux hypothèses importantes : d'abord la distance qui sépare les deux parois est grande devant l'épaisseur visqueuse δ_v , ensuite la température moyenne dans le fluide est uniforme. Ces deux hypothèses ne sont pas applicables à l'espace séparant deux plaques de l'empilement d'un réfrigérateur thermoacoustique. En effet la distance $2y_0$ entre ces plaques est de l'ordre de grandeur de l'épaisseur visqueuse, δ_v , et un gradient moyen de température est présent. Plusieurs auteurs ont calculé analytiquement les mouvements moyens du second ordre entre deux parois en relâchant les hypothèses de Rayleigh [5–7]. Le présent travail vient compléter ces analyses tout en ne faisant aucune hypothèse simplificatrice. Tout d'abord, quand une séparation importante des plaques est choisie ($y_0/\delta_v = 32$), les caractéristiques essentielles de l'analyse de Rayleigh sont retrouvées. Quatre tourbillons moyens sont présents dans le canal séparant deux plaques de l'empilement : deux tourbillons « intérieurs » de couche limite situés près des parois, et deux tourbillons « extérieurs » situés au centre du canal (Fig. 4 et Fig. 5(a)). Quand la valeur du paramètre y_0/δ_v décroît les tourbillons extérieurs diminuent en taille (Figs. 6 cas $y_0/\delta_v = 8$, et Fig. 5(b)) puis disparaissent lorsque y_0/δ_v est de l'ordre de 5. Seuls les tourbillons intérieurs demeurent alors (Fig. 6 cas $y_0/\delta_v = 4$, $y_0/\delta_v = 3$, et Fig. 5(c)). Lorsque la valeur de y_0/δ_v est encore réduite et atteint approximativement l'unité, les tourbillons « intérieurs » disparaissent à leur tour, laissant place à un écoulement moyen uniforme dirigé vers le ventre de vitesse (Fig. 6 cas $y_0/\delta_v = 0,75$ et $y_0/\delta_v = 0,5$, et Fig. 5(d)). Les comportements sont qualitativement identiques pour les plaques isotherme et adiabatique. Toutefois la disparition des tourbillons extérieurs puis intérieurs se produit de façon plus précoce pour une plaque isotherme. Les comportements trouvés ici sont qualitativement en accord avec les résultats analytiques de Hamilton et al. [7] obtenus pour un résonateur entier.

1. Introduction

A thermoacoustic refrigerator is shown in Fig. 1. It consists of an acoustic source, a resonator whose length l_{res} is one-half the wave length, λ , a stack of plates located at $x = x_S$, and two heat exchangers [1]. The source and the resonator create an intense standing wave. The interaction of this wave with the plates of the stack results in heat

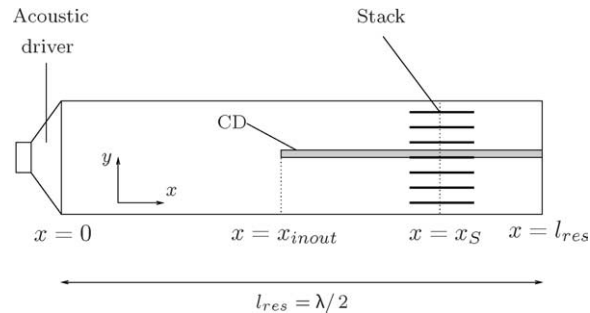


Fig. 1. Sketch of a thermoacoustic refrigerator. Domain CD is the computational domain.

Fig. 1. Schéma d'un réfrigérateur thermoacoustique. CD est le domaine de simulation.

pumping from one extremity of the plates to the other. The heat pumped by the stack is then taken out of the cold heat exchanger connected to the reservoir to be cooled, and released to the hot heat exchanger. Thermoacoustic refrigerators have a few advantages: in particular, they are reliable and may be miniaturized. However, their efficiency still needs to be improved and their performance needs to be better understood. Among the factors that are still poorly understood are the mean (time-averaged) flows in the device. Some previous studies have investigated the problem of streaming in the case of thermoacoustic engines in which a close loop is present [2]. Streaming in standing wave devices, such as the refrigerator shown in Fig. 1, has received little attention. It is the subject of the present Note.

The first calculation of streaming induced by standing wave between parallel walls is due to Rayleigh [3]. Two major assumptions were made by Rayleigh in his calculation: (i) the wall separation distance is large compared to the viscous boundary layer thickness; (ii) the mean temperature is uniform. These assumptions preclude the application of Rayleigh's models to thermoacoustic devices stacks, whose plates are separated by a distance on the order of the viscous boundary layer thickness, and which feature large mean temperature gradients. In other early models for thermoacoustic phenomena, Rott [4] included the effect of a mean temperature gradient, keeping the large wall-separation approximation. Recent analytical work by Waxler [5], Bailliet et al. [6], and Hamilton et al. [7] have addressed the problem of streaming between parallel walls with an arbitrary separation distance and/or in the presence of a mean temperature gradient. Also large amplitude streaming has been considered by Menguy and Gilbert [8] and Yano [9]. Such streaming may arise in thermoacoustic resonators usually driven at large amplitudes.

The present Note is devoted to streaming in the vicinity of a thermoacoustic stack, where the plate separation distance is arbitrary, and where edge effects are expected due to the finite length of the plate. The numerical model of the problem is presented in Section 2. Results for the mean flow field are presented in Section 3. Two regions are distinguished. One region consists of the areas located at the plate extremities, where the mean flow is due to the abrupt change from a slip condition to a no-slip condition. Another region is located near the plate center. In this region a second-order streaming flow pattern is observed. The effects of channel height on this flow is studied in Section 4.

2. Numerical model

The velocity field in the vicinity of the stack was calculated by solving the two-dimensional, unsteady, compressible, Navier–Stokes equations. The energy equation was also solved both for the stack and the fluid. The computational domain CD is shown in Figs. 1 and 2. The fluid considered is air. Due to the stack periodicity, only one plate is included in the domain and symmetric lateral boundary conditions are used. The plate is thin (its thickness is zero). Two thermal boundary conditions were imposed, in turn, on the plate surface: an isothermal condition (the temperature of the fluid has a fixed imposed value on the plate surface), and an adiabatic condition (no heat

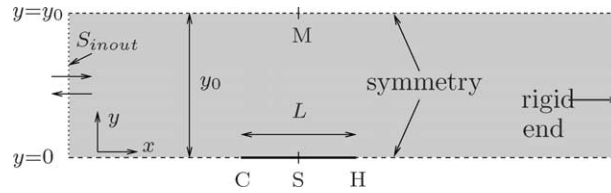


Fig. 2. Computational domain CD.

Fig. 2. Domaine de simulation CD.

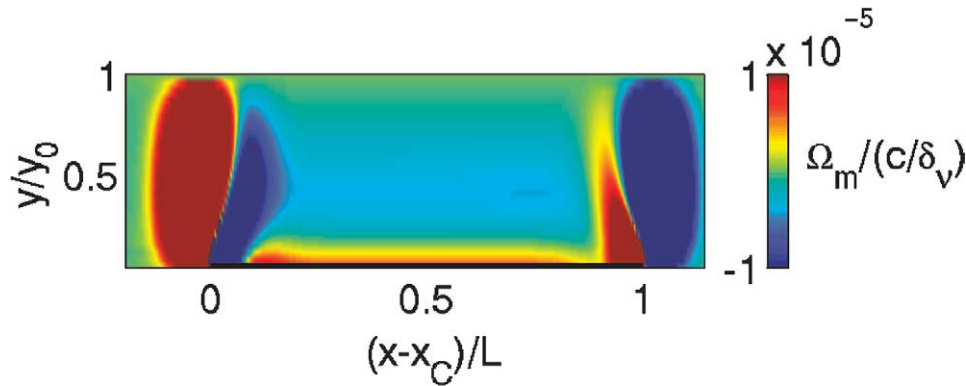


Fig. 3. Mean vorticity field in the vicinity of the stack plate.

Fig. 3. Champ de vorticit  moyenne aux alentours de la plaque.

flux into the plate). The plate, of length L , is located at position x_S (see Fig. 1), expressed in nondimensional form as kx_S , where $k = 2\pi/\lambda$ is the wave number. The height, y_0 , of the domain is one-half the plate separation distance, $2y_0$, within the stack. The dimensionless form y_0/δ_v is also used, where the viscous boundary layer thickness is defined by $\delta_v = \sqrt{2\nu/\omega}$ (ν is the kinetic viscosity and ω is the angular frequency).

A travelling wave was introduced into the computational domain through the boundary S_{inout} , using the method of characteristics. This wave travels through the domain and is reflected at the resonator rigid end. The sum of the incident and reflected waves forms the imposed standing wave. The amplitude of the wave is given by the Mach number, defined by $M_a = u_A/c$, where u_A is the maximal amplitude of the velocity in the resonator, and c is the speed of sound.

The time integration is performed using a fourth-order Runge–Kutta method and spatial derivatives are calculated using fourth order finite differences. To reduce computational effort, the frequency, f , of the source was relatively high, $f = 20$ kHz. More details about the simulations are given in [10].

3. Mean velocity field

The parameters of the simulation are as follows: $L = \lambda/40$, $kx_S = 2.35$, $y_0/\delta_v = 3$ and $M_a = 0.005$. An isothermal boundary condition was imposed. The mean (time-averaged) vorticity field, Ω_m , is shown in Fig. 3. Two regions can be identified. The first region consists of the two extremities of the plate, where vortical mean motions occur. The second region is located above the mid part of the plate. The norm of the vorticity is much more important in the first region than in the second. Moreover, the vorticity is proportional to the Mach number, M_a , in the first region while it is proportional to the square of the Mach number, M_a^2 , in the second region. The mean vortical motions that occur in the first region are due to the change from a slip condition just outside the plate to a

non-slip condition on the plate surface. Such mean vortical motions at each edge of the plate are also mentioned by Ishikawa and Mee [11]. As can be seen from Fig. 3, these mean motions are coupled to those in the second region. The mean velocity field in the second region corresponds to what is usually called ‘acoustic streaming’, and results from the interaction of the sound field with the plate boundaries.

4. Streaming flow above the mid part of the plate

The streaming flow above the mid part of the plate is now studied in more details. The x -component of the mean velocity, u_m , is computed in the section SM of the domain located above the plate (see Fig. 2). Here, u_m represents the Eulerian mean velocity.

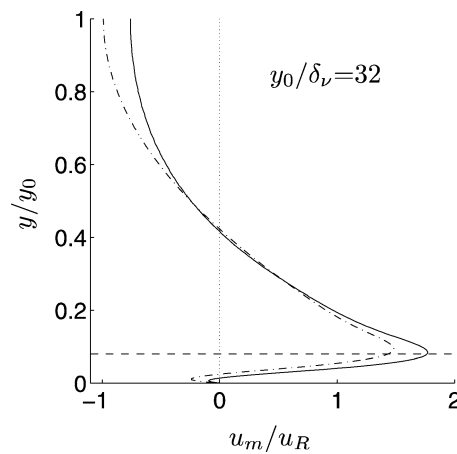


Fig. 4. Mean axial velocity u_m in section SM of the computational domain. — simulation, — Eq. (1). The velocity is made dimensionless using the Rayleigh velocity $u_R = 3u_A^2/16c$. The horizontal dashed line (---) represents the limit between the inner and the outer vortices.

Fig. 4. Vitesse axiale moyenne u_m dans la section SM du domaine de calcul. — simulation, — Eq. (1). u_m est adimensionnée par la vitesse de Rayleigh $u_R = 3u_A^2/16c$. La ligne interrompue horizontale (---) marque la limite entre les tourbillons intérieurs et extérieurs.

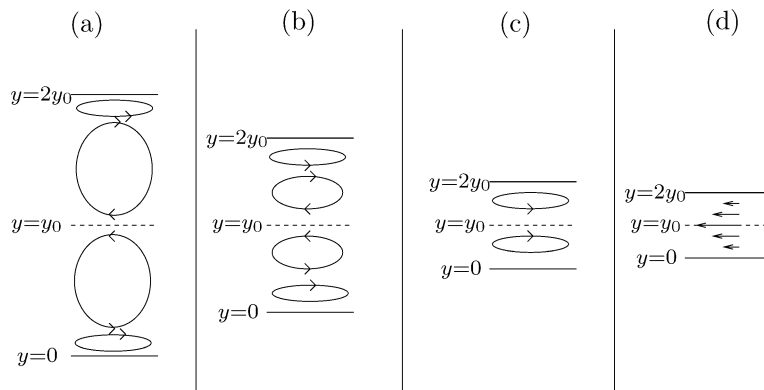


Fig. 5. Qualitative sketch of the streamlines of the mean Eulerian velocity u_m in the space between two plates in the stack. Only the part $0 < y < y_0$ is calculated in the present simulation, the part $y_0 < y < 2y_0$ being obtained by symmetry. From (a) to (d) the ratio y_0/δ_ν decreases.

Fig. 5. Tracé qualitatif des lignes de courant pour la vitesse moyenne eulérienne u_m dans l’espace inter-plaques de l’empilement. Seule la partie $0 < y < y_0$ est calculée dans la simulation, la partie $y_0 < y < 2y_0$ est obtenue par symétrie. De (a) à (d) le rapport y_0/δ_ν diminue.

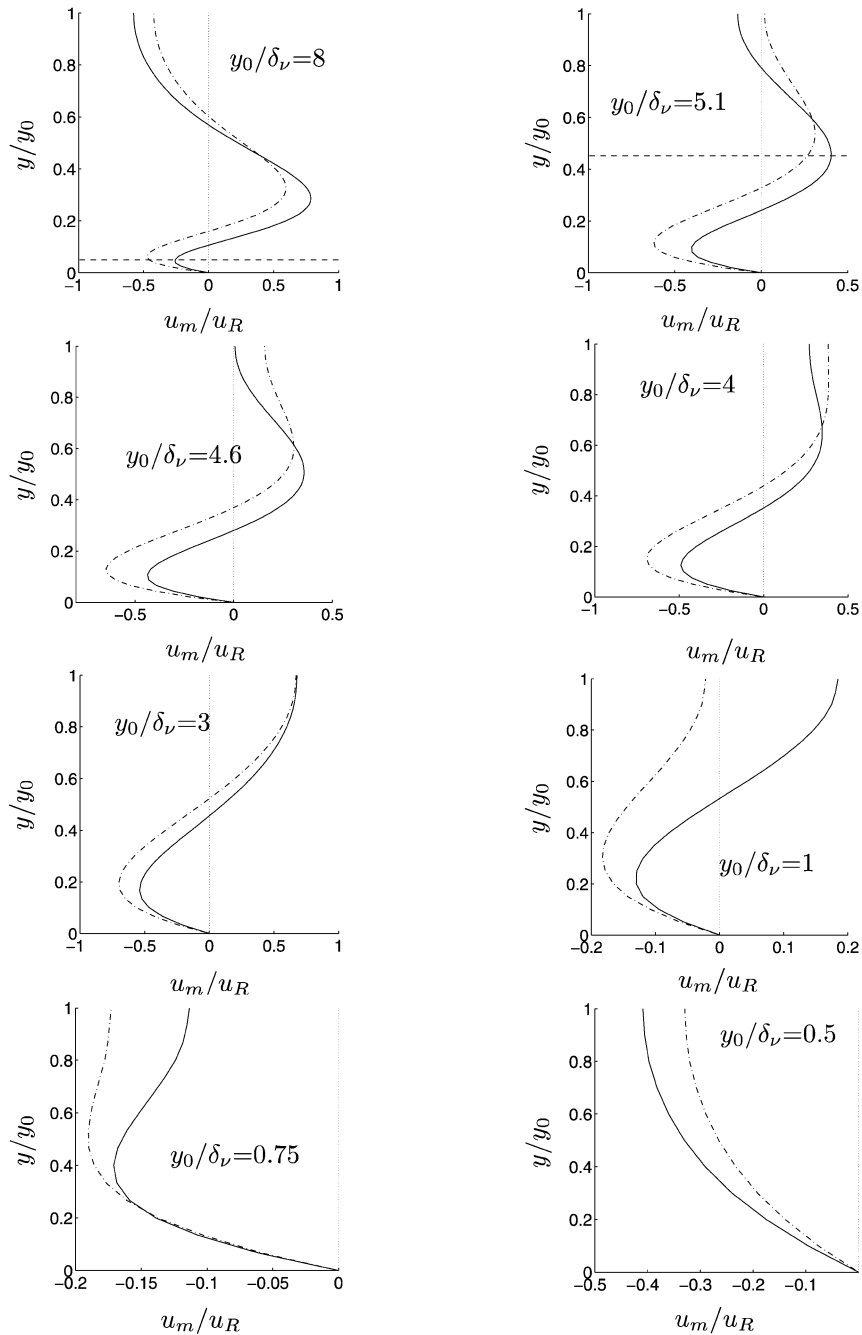


Fig. 6. Mean axial velocity u_m in section SM of the computational domain, for several values of y_0/δ_ν : — isothermal plate, - - - adiabatic plate. u_m is made dimensionless using the Rayleigh velocity $u_R = 3u_A^2/16c$. The horizontal dashed line (- -), when present, represents the limit between the inner and the outer vortices for the isothermal plate.

Fig. 6. Vitesse moyenne u_m dans la section SM du domaine de calcul, pour plusieurs valeurs de y_0/δ_ν : — plaque isotherme, - - - plaque adiabatique. u_m est adimensionnalisée par la vitesse de Rayleigh $u_R = 3u_A^2/16c$. L'éventuelle ligne interrompue horizontale (- -) marque la limite entre les tourbillons extérieurs et intérieurs pour la plaque isotherme.

First, a comparison with the early work of Rayleigh on acoustic resonators is made. The mean velocity first calculated by Rayleigh and then slightly modified by Nyborg (correction for the boundary layer) is [12]:

$$u_m(x, y) = \frac{u_A^2}{8c} \sin(2kx) (F_1(y) + 3 - 18F_2(y)) \quad (1)$$

where $F_1(y)$ et $F_2(y)$ are given by:

$$F_1(y) = -\left(e^{-2y/\delta_v} + 2e^{-y/\delta_v} \cos\left(\frac{y}{\delta_v}\right) + 6e^{-y/\delta_v} \sin\left(\frac{y}{\delta_v}\right) \right), \quad F_2(y) = \frac{y}{2y_0} \left(1 - \frac{y}{2y_0} \right) \quad (2)$$

This formula can be used only for channels that are wide compared to the viscous boundary layer thickness. Hence, a large value $y_0/\delta_v = 32$ is used. The values of the other parameters are: $L = \lambda/20$, $kx_S = 2.43$, $Ma = 0.001$. The mean velocity in section SM predicted by the numerical simulation and Eq. (1) are plotted in Fig. 4. Note that a perfect agreement is not expected for two reasons. Rayleigh's solution does not take into account the mean temperature gradient that appears in the present simulation due to the thermoacoustic heat pumping. Furthermore Rayleigh's solution is obtained in the case of a resonator, which corresponds to a situation for which the entire bottom boundary of the domain CD would be a wall, in contrast with the present simulation which includes a plate over only on a portion of that boundary. Nevertheless, the results from the simulation and those from Eq. (1) are close. In particular, the mean velocity, u_m , changes sign twice in the section, that is four times in the space between two plates (due to symmetry). Thus, as illustrated in Fig. 5(a) four mean vortices are present between the plates. Two small vortices, usually referred to as 'inner vortices', are located in the boundary layers near the plates, and two other much bigger vortices, usually referred to as 'outer vortices', are located in the core of the channel between the plates. In Fig. 4, the horizontal dashed line represents the limit between the inner and outer vortices.

Smaller values of y_0/δ_v are now considered, which correspond to realistic values for the plate spacing in a thermoacoustic stack. Parameters for this simulation are: $L = \lambda/40$, $Ma = 0.01$, $kx_S = 2.43$. y_0/δ_v takes eight values between 8 and 0.5. The mean velocity along section SM is given for the different values of y_0/δ_v in Fig. 6, for both an isothermal and an adiabatic boundary condition on the plate surface. The case of the isothermal plate is first discussed. For $y_0/\delta_v = 8$ and $y_0/\delta_v = 5.1$, the mean velocity changes sign twice in the section, indicating the presence of four vortices between the two plates. The size of the outer vortices decreases as y_0/δ_v decreases, which corresponds to a transition from sketch (a) to sketch (b) in Fig. 5. For $y_0/\delta_v = 4.6$, the velocity changes sign only once within the section. Thus, the outer vortices have disappeared, and only the two inner vortices remain in the plate interspace, as illustrated in Fig. 5(c). If the value of y_0/δ_v is decreased further, the mean velocity distribution is changed, and below a certain value, the mean velocity has a constant sign across the section (cases $y_0/\delta_v = 0.75$ and $y_0/\delta_v = 0.5$ in Fig. 6 and sketch (d) in Fig. 5). For an adiabatic condition, a similar qualitative behaviour is obtained but transitions occur for different values of y_0/δ_v . In particular, the new value $y_0/\delta_v = 5.1$ for which outer vortices disappear is larger than the corresponding value $y_0/\delta_v = 4.6$ for an isothermal condition. The previous values were given in terms of the Eulerian velocity. In terms of the mean mass transport velocity (see [7]), it appears that outer vortices disappear when $y_0/\delta_v = 5.7$ for an adiabatic condition, and when $y_0/\delta_v = 5.2$ for an isothermal condition.

These results agree qualitatively well with the analytical work of Hamilton et al. [7] who calculated the streaming in an entire resonator with small wall separation, and for an isentropic flow. In particular, the separation, $2y_0$, for which the outer vortices disappear in their study (in terms of the mean mass transport velocity) corresponds to $y_0/\delta_v = 5.7$, a value equal to that found in the present work. This agreement is rather unexpected, and shows that the theory of Hamilton et al. [7] may indeed be used to calculate the streaming inside a thermoacoustic stack, at least for moderate Mach numbers.

5. Conclusion

The mean velocity field in the vicinity of a thermoacoustic stack plate was calculated. Two regions were distinguished. At the plate extremities, time averaged vortical motion were observed, due to the abrupt change from slip to non-slip conditions at the plate edges. Above the plate center, time-averaged motion corresponding to classical acoustic streaming patterns were found. When the plates separation was reduced to about ten boundary layer thicknesses, the outer vortices predicted by Rayleigh's theory disappeared. Only two inner vortices were present, which also disappear when the plates separation became less than about one viscous boundary layer thickness. Also it was noticed that the thermal condition at the plate (isothermal/adiabatic), has a slight but non-negligible effect on acoustic streaming phenomena.

Acknowledgements

This work was supported by Délégation Générale pour l'Armement (DGA), French ministry of Defense.

References

- [1] G.W. Swift, Thermoacoustics engines, *J. Acoust. Soc. Am.* 84 (1988) 1145–1180.
- [2] S. Backhaus, G.W. Swift, A thermoacoustic-Stirling heat engine: detailed study, *J. Acoust. Soc. Am.* 107 (2000) 3148–3166.
- [3] J.W. Rayleigh, On the circulation of air in Kundt's tube, and on some allied acoustical problems, *Philos. T. Roy. Soc.* 175 (1883) 1–21.
- [4] N. Rott, The influence of heat conduction on acoustic streaming, *Z. Angew. Math. Phys.* 25 (1974) 417–421.
- [5] R. Waxler, Stationary velocity and pressure gradients in a thermoacoustic stack, *J. Acoust. Soc. Am.* 109 (2001) 2739–2750.
- [6] H.A. Bailliet, V. Gusev, R.A. Hiller, Acoustic streaming in closed thermoacoustic devices, *J. Acoust. Soc. Am.* 110 (2001) 1808–1821.
- [7] M.F. Hamilton, Y.A. Ilinskii, E.A. Zabolostkaya, Acoustic streaming generated by standing waves in two-dimensional channels of arbitrary width, *J. Acoust. Soc. Am.* 113 (2003) 153–160.
- [8] L. Menguy, J. Gilbert, Non-linear acoustic streaming accompanying a plane stationary wave in a guide, *Acta Acust.* 86 (2000) 249–259.
- [9] T. Yano, Turbulent acoustic streaming excited by resonant oscillation shock waves in a closed tube, *J. Acoust. Soc. Am.* 106 (1999) L7–L12.
- [10] D. Marx, Ph. Blanc-Benon, Numerical simulation of the coupling between stack and heat exchangers in a thermoacoustic refrigerator, in: 9th AIAA-CEAS Aeroacoustic Conference, Hilton Head, SC, USA, 12–14 May, 2003, AIAA Paper 2003–3150.
- [11] H. Ishikawa, D.J. Mee, Numerical investigations of flow and energy fields near a thermoacoustic couple, *J. Acoust. Soc. Am.* 111 (2002) 831–839.
- [12] W.L. Nyborg, Acoustic streaming, in: W.P. Mason (Ed.), *Physical Acoustics*, Academic Press, New York, 1965, pp. 265–331, vol. 2B, Chapter 7.